Plant Pathology

WILEY

Plant Pathology

ORIGINAL ARTICLE OPEN ACCESS

Dose Splitting Increases Selection for Both Target-Site and Non-Target-Site Fungicide Resistance—A Modelling Analysis

Isabel Corkley[1,2,3] | Alexey Mikaberidze[2] | Neil Paveley[4] | Frank van den Bosch[5,6] | Michael W. Shaw[2] | Alice E. Milne[1]

[1]Net Zero and Resilient Farming, Rothamsted Research, Harpenden, UK | [2]School of Agriculture, Policy and Development, University of Reading, Reading, UK | [3]Sustainable Agricultural Systems, ADAS, Wolverhampton, UK | [4]Sustainable Agricultural Systems, ADAS, High Mowthorpe, UK | [5]Quantitative Biology and Epidemiology Group, Plant Pathology Department (Visiting Scholar), University of California, Davis, Davis, California, USA | [6]Sustainable Agricultural Systems, ADAS, Hereford, UK

Correspondence: Isabel Corkley (isabel.corkley@rothamsted.ac.uk; isabel.corkley@adas.co.uk)

Received: 6 August 2024 | **Revised:** 23 January 2025 | **Accepted:** 8 February 2025

Funding: This work was supported by Biotechnology and Biological Sciences Research Council (BBS/E/RH/230003C) and Agriculture and Horticulture Development Board (21120062).

Keywords: epidemiological model | fungicide resistance management | non-target-site resistance | partial resistance | quantitative resistance | Septoria tritici blotch

ABSTRACT

Fungicide resistance management principles recommend that farmers avoid splitting the total dose applied of a fungicidal mode of action (MoA) across multiple applications per season ('dose splitting'). However, dose splitting may sometimes be needed to make another proven resistance management tactic—application in mixture with a different MoA—practically achievable, especially in cases where there are limited MoAs available for disease control. Variable effects of dose splitting on selection for resistance have been observed in field experiments, and its effect on selection for partial resistance in fungal pathogens is not well studied. An improved understanding of whether the effect of dose splitting depends on fungicide properties and the type of fungicide resistance is required. We developed a compartmental epidemiological model of Septoria leaf blotch (STB) (*Zymoseptoria tritici*) to investigate the effect of dose splitting on selection for both complete and partial target-site and non-target-site resistance. To solely measure the effects of dose splitting, we restricted the analysis to solo fungicide application (solo use is not recommended in practice). Our results show variable effects of dose splitting: in general, it increased the selection for both target-site and non-target-site resistance. Within the range of dose–response parameters expected for commercial fungicides, dose splitting increased the selection most for partial resistance mechanisms that result in a reduction in fungicide efficacy at low fungicide concentrations but not at high concentrations. We predict that dose splitting of a succinate dehydrogenase inhibitor (SDHI) fungicide (solo) will increase selection for target-site and non-target-site resistance by between 20% and 35%, respectively.

1 | Introduction

The effectiveness of fungicides for control of plant diseases is threatened by the evolution of resistance (Corkley et al. 2022). The risk of resistance is particularly high for polycyclic foliar fungal pathogens, such as Septoria tritici blotch (STB) (*Zymoseptoria tritici*) in wheat, grey mould (*Botrytis cinerea*) in many hosts, potato late blight (*Phytophthora infestans*), and net blotch (*Pyrenophora teres*) and powdery mildew (*Blumeria hordei*) diseases of barley. These pathogens have large

population sizes and many generations per year, enabling rapid evolution of resistance (Grimmer et al. 2015; McDonald et al. 2022), and have the potential to cause large economic losses. Fungicide resistance management tactics include minimising the dose and number of applications and applying in mixture with a different mode of action (MoA) (Corkley et al. 2022; Elderfield et al. 2018; Mikaberidze et al. 2017; van den Berg et al. 2016; van den Bosch, Oliver, et al. 2014; van den Bosch, Paveley, et al. 2014). However, the number of effective MoAs available for use is increasingly restricted by regulation (especially of multisite fungicides) and resistance that has already evolved. This poses challenges for the implementation of current resistance management strategies.

Fungicides with an MoA affecting a single pathogen target site are at a particular risk of resistance development because one or more mutations affecting the target-site gene ('target-site resistance') can confer a large fitness advantage. For example, the G143A mutation prevents quinone outside inhibitor (QoI) fungicides from binding to the cytochrome b mitochondrial protein, restoring its function in respiration (Dorigan et al. 2023). *Z. tritici* has accumulated multiple mutations in the *CYP51* gene, each conferring partial resistance but in combination causing gradually increasing levels of resistance to demethylation inhibitor (DMI) fungicides (Cools and Fraaije 2013; Hawkins and Fraaije 2021; Leroux and Walker 2011). In addition to target-site mutations, other mechanisms of fungicide resistance in pathogens include target-site overexpression and non-target-site resistance, such as increased efflux, detoxification and alternative metabolism (Dorigan et al. 2023; Hawkins and Fraaije 2021; Hu and Chen 2021). These mechanisms generally cause partial resistance, although they may cause more highly resistant strains when in combination with target-site resistance. Metabolic resistance pathways such as efflux pumps are also implicated in multidrug-resistant fungal strains (Kretschmer et al. 2009; Omrane et al. 2017; Patry-Leclaire et al. 2023).

To predict the impact of fungicide resistance management tactics on selection, it is helpful to consider pathogen epidemics in terms of the per capita rate of increase or 'growth rate' (r) of each strain. This approach combines the repeating stages of lesion establishment, growth and sporulation into a single measure of the success of a strain at a given point in time. When a fungicide is applied, the growth rates of pathogen strains with resistance to the action of a fungicide are higher than those of strains that are sensitive to the fungicide. The greater the difference in the per capita growth rates of resistant and sensitive strains, the faster the rate of selection for resistance (van den Bosch, Oliver, et al. 2014). The impact of any given fungicide dose on the per capita growth rate of a pathogen strain can be represented in models by its effect on important parts of the pathogen life cycle, such as a reduction in the pathogen transmission rate. Assuming that the applied dose decays exponentially over time, it is possible to track the 'effective dose' remaining at any point in time. The impact of the fungicide on the pathogen life cycle is greatest at high effective doses, where the maximum effect is defined by an 'asymptote parameter', and the rate at which the effect decreases with reducing fungicide doses is defined by a 'curvature parameter'. Resistance will cause a change in the dose–response to a fungicide, which may be apparent either as a complete or partial reduction in the maximum effect of the fungicide on the pathogen growth rate even at high effective doses, or as a reduction in the efficacy of lower effective doses of the fungicide. We will refer to these types of resistance as 'asymptote shift' and 'curvature shift' respectively, to reflect their effect on the fungicide dose–response (Figure 1a,b). Resistance resulting from an asymptote shift is sometimes referred to as 'qualitative' or 'type I' resistance, and resistance resulting from a curvature shift as 'quantitative' or 'type II' resistance (Elderfield 2018; Mikaberidze et al. 2017; Taylor and Cunniffe 2023a).

Let us consider which resistance mechanisms are likely to lead to either a partial asymptote shift or a curvature shift. Some fungicides bind competitively directly to the enzyme active site: for example, DMI fungicides bind competitively to the CYP51 protein, which catalyses a step in ergosterol biosynthesis (Hargrove et al. 2015), occupying the P450 active site and preventing substrate binding. A target-site mutation that causes a small to moderate reduction in the affinity of the enzyme for the fungicide will reduce fungicide efficacy at low fungicide concentrations but not at high fungicide concentrations. This case is therefore best represented by a curvature shift. A curvature shift will also be representative of other resistance mechanisms that reduce fungicide efficacy at low fungicide concentrations but are overwhelmed by high fungicide concentrations. These may include target-site overexpression and non-target-site metabolic resistance mechanisms such as increased expression of efflux pumps and detoxification. A partial asymptote shift could result from a target-site mutation that reduces the maximum effect of fungicides, which bind allosterically and non-competitively to an enzyme. These fungicides change the structure of the enzyme in a way that inhibits enzyme function or reduces access to or binding of the substrate to the enzyme active site. An example is the cyanoacrylate phenamacril, which is used against a number of *Fusarium* species (Wollenberg et al. 2020). The maximum effect of these fungicides could be partially reduced by a target-site mutation that changes the shape of the enzyme–fungicide complex, partially restoring enzyme function.

Multiple fungicide applications per year are often useful for control of polycyclic foliar fungal pathogens. If the number of MoAs available for programmes is limited, use of mixtures may require splitting the total dose of a fungicide across two or more applications, reducing the dose of each MoA per application but increasing the exposure time of the pathogen to each fungicide, with counteracting (but not necessarily equal) effects on selection for resistance. If resistance is evolving 'concurrently' to two or more MoAs at the same time, there are complex trade-offs for resistance management. Whether 'splitting and mixing' is a useful strategy for management of concurrent evolution of resistance will depend on the balance between the effects of mixture and dose splitting on selection. However, variation in the effects of dose splitting has been observed in field trials (Paveley et al. 2020; Young et al. 2021) and is not well understood. van den Bosch, Oliver, et al. (2014) hypothesise that dose splitting will increase selection overall for strains with an asymptote shift and highlight several experimental studies that support this theory. The effect of dose splitting on selection for partially resistant strains with a curvature shift has not been explicitly considered

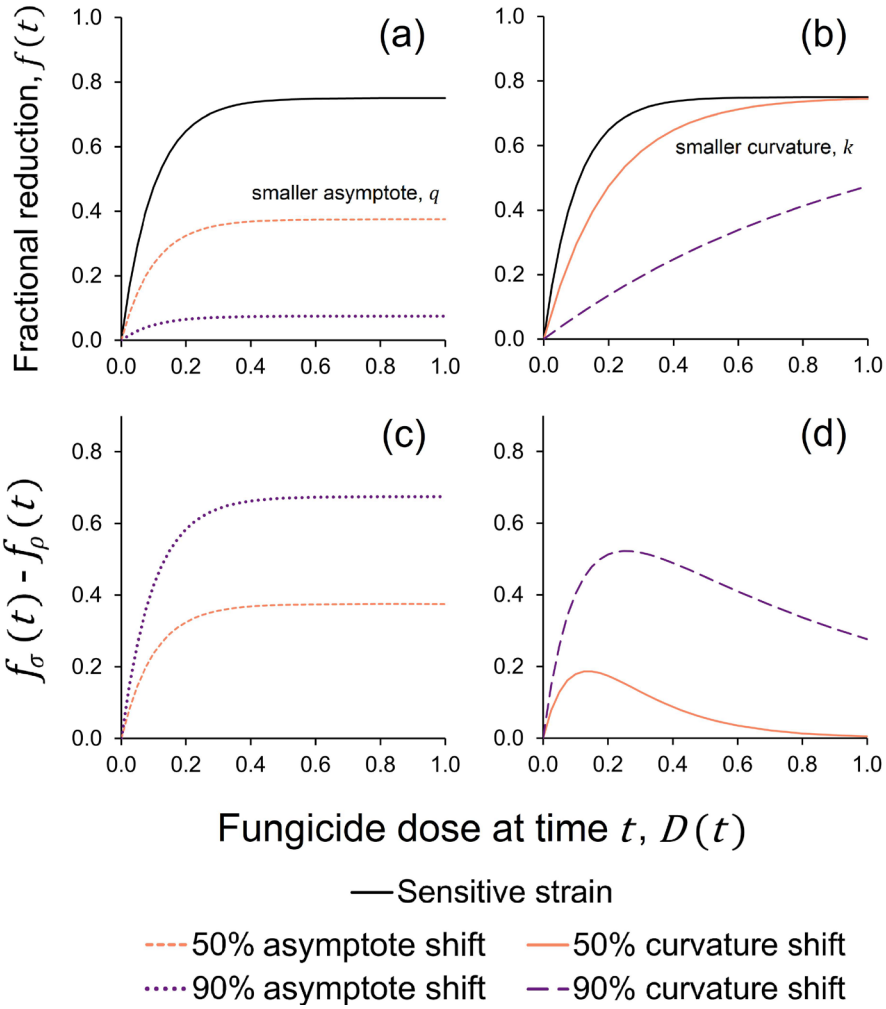

FIGURE 1 | Effect of asymptote shift, ζ_q, and curvature shift, ζ_k, on the dose–response to fungicide dose, $D(t)$. Panels (a) and (b) show the fractional reduction, $f(t)$, of pathogen life cycle parameters for different levels of asymptote shift and curvature shift, respectively. Panels (c) and (d) show $f_\sigma(t) - f_\rho(t)$, the resulting difference in $f(t)$ of the sensitive strain compared to that of a resistant strain with an asymptote shift or a curvature shift, respectively. Dose–response shown for a fungicide with $q_\sigma = 0.75, k_\sigma = 10$. [Colour figure can be viewed at wileyonlinelibrary.com]

in previous modelling studies. An improved understanding of how fungicide properties and type of resistance determine the effect of dose splitting on selection for resistant pathogen strains is needed to inform management tactics.

To investigate the effect of dose splitting on selection, we developed a model of fungicide resistance evolution in *Z. tritici*. *Z. tritici* is one of the most common and damaging pathogens affecting winter wheat crops in the UK and worldwide, associated with a reduction in crop quality and yield losses of up to 50% if uncontrolled (Fones and Gurr 2015). It has evolved resistance to QoIs, DMIs and SDHIs (Cools and Fraaije 2013; Dooley et al. 2016; Huf et al. 2018; Rehfus et al. 2018; Torriani et al. 2009), with a corresponding decline in disease control (Blake et al. 2018). The model simulates a typical UK epidemic of STB, describing the seasonal growth and senescence of the upper crop canopy of winter wheat under average temperature conditions in the UK, key processes in the pathogen life cycle (sporulation, infection and growth) and their interaction with fungicides. In the UK, initial infection of wheat crops by *Z. tritici* occurs in autumn or spring through airborne ascospores or by splash-dispersed conidia from wheat stubble. The fungus develops slowly during a symptomless latent period, following which necrotic lesions form on the leaf surface. These produce asexual haploid pycnidiospores that spread to the upper leaf canopy through contact and rain splash, driving the majority of secondary infections within the growing season (Ponomarenko et al. 2011; Suffert et al. 2011).

Through model simulations, we compared the effects on selection for a resistant *Z. tritici* strain of applying a fungicide solo in either a single application at full label rate or in two applications, each at half the full label rate. It should be noted that use of a solo MoA is not recommended in practice. However, restricting the analysis to dose splitting of a solo fungicide enabled us to measure solely the effects of dose splitting, rather than the combined effects of 'splitting and mixing', giving a clearer picture of the drivers in variation of the effects of dose splitting. We used the model to investigate how the effect of dose splitting on selection for resistance depends on (a) fungicide properties (foliar concentration half-life; asymptote and curvature dose–response parameters for the sensitive strain); (b) the type of resistance

(asymptote shift or curvature shift); and (c) the magnitude of the asymptote or curvature shift.

2 | Materials and Methods

2.1 | Model Background and Approach

We follow the approach of Hobbelen, Paveley, and van den Bosch (2011), modelling the leaf area index (LAI; a dimensionless measure of leaf density, defined as the total amount of one-sided leaf area of the canopy [m^2] per unit ground area [m^2]) and infection by *Z. tritici* pycnidiospores on the top three leaves of the wheat canopy only. Yield loss due to *Z. tritici* occurs due to a reduction in healthy leaf area duration (HAD) and the resulting loss of interception of photosynthetically active radiation (PAR) on the upper three leaves during grain filling; the level of disease on the upper canopy is a good predictor of yield loss (Parker et al. 2004; Shaw and Royle 1989). Fungicide applications targeted against *Z. tritici* are therefore mostly applied to the upper leaf canopy. Although there will be some fungicide exposure on lower leaves, previous modelling results suggest that it is on the upper leaf canopy that selection for resistance primarily occurs (van den Berg et al. 2013).

The dynamics of the epidemic in the model are driven by the growth and senescence of the crop, which determines the leaf area available for infection, and the effect of a fungicide on the pathogen life cycle over time. The leaf area can pass sequentially through healthy, latent (infected but not yet sporulating), infectious (sporulating) and post-infectious stages; healthy and latent leaf area may also senesce due to leaf age. The infectious leaf area generates new infections on healthy leaf area. The model simulates the LAI of both the latent and infectious stages of a sensitive strain and a resistant strain of *Z. tritici*.

Our model has the same functional form as the one developed by Hobbelen, Paveley, Fraaije et al. (2011) and Hobbelen, Paveley, and van den Bosch (2011). However, the rate of senescence in that model was parameterised using data on spring barley (*Hordeum vulgare*) (Hobbelen, Paveley, Fraaije et al. 2011), and the simulated timing of crop senescence could impact on model predictions of the effects of dose splitting on selection for resistant strains. We therefore reparameterised the model (see Section 2.3) using a dataset of green leaf area index (GLAI) and *Z. tritici* infection of the top three leaves of wheat crops from 14 site-years (Milne et al. 2003, described as 'Data set 1'; te Beest et al. 2009).

2.2 | Model Equations

2.2.1 | Growth and Senescence of Wheat Leaf Canopy

It is assumed that the growth rate of the total leaf area of the upper canopy is not affected by *Z. tritici* severity, so the total LAI and uninfected healthy GLAI are tracked separately (Hobbelen, Paveley, and van den Bosch 2011). In the absence of disease, the rates of change of the total LAI (A) and the total healthy GLAI (H) are given by

$$\frac{dA}{dt} = \begin{cases} 0, & t < t_0 \\ \gamma\left(A_{\text{Max}} - A\right), & t > t_0 \end{cases} \quad (1)$$

$$\frac{dH}{dt} = \gamma\left(A_{\text{Max}} - A\right) - \beta(t)H \quad (2)$$

$$\text{where } \beta(t) = \begin{cases} 0, & t < t_{\beta_0} \\ \tau\left(\dfrac{t - t_{\beta_0}}{t_{\beta_T} - t_{\beta_0}}\right) + \varphi e^{\omega\left(t_{\beta_T} - t\right)}, & t_{\beta_0} \le t \le t_{\beta_T} \end{cases} \quad (3)$$

where t_0 is the time at which leaf 3 emerges and the growth of the upper canopy commences, A_{Max} is the maximum LAI, γ is the growth rate of the leaf area, $\beta(t)$ is the rate of senescence at time t, t_{β_0} is the time of onset of senescence, t_{β_T} is the time at which the canopy has fully senesced and τ, φ and ω are the coefficients controlling the rate at which senescence occurs in relation to the length of time after the onset of senescence. Time is measured in degree days (base 0°C, 'zero-degree days'; see Section 2.3).

2.2.2 | Infection of Crop by *Z. tritici*

The development of the STB epidemic is described in the model by tracking the LAI of latent and infectious lesions of the resistant and sensitive strains.

It is assumed that the epidemic on the upper leaves is initiated by an influx of spores from infectious lesions on lower leaves. The density of infectious lesions on lower leaves, C, diminishes over time at rate λ, as lower leaves senesce and infectious lesions on the lower leaves reach the end of the infectious period. The LAI of infectious lesions on lower leaves at time t, $C(t)$, is calculated as

$$C(t) = C_0 e^{-\lambda t} \quad (4)$$

A fraction, $\theta_{\rho_{\text{Start}}}$, of the initial influx C from lower leaves is assumed to be spores of the resistant strain, with the sensitive strain fraction $\theta_{\sigma_{\text{Start}}} = 1 - \theta_{\rho_{\text{Start}}}$. It is assumed that $\theta_{\rho_{\text{Start}}}$ and $\theta_{\sigma_{\text{Start}}}$ are not affected by fungicide application after the start of the model simulation at growth stage (GS) 31. The initial influx is denoted as C_σ and C_ρ for the sensitive and resistant strains, respectively.

The influx of spores, C, and infectious LAI on the upper canopy, I, are converted into new latent lesions on the upper canopy, at transmission rate ε, that is, the overall rate at which infectious lesion density is converted into new latent lesions on a given density of healthy leaf area. Latent lesions mature into infectious, sporulating lesions, at a rate δ, where $1/\delta$ is the average latent period. Infectious lesions die at a rate μ, where $1/\mu$ is the average infectious period. Leaf senescence affects latent LAI, but not infectious LAI as the leaf tissue is already killed by the necrotic process of lesions becoming infectious (Hobbelen, Paveley, and van den Bosch 2011; Kema et al. 1996). The following set of equations track the area index of healthy (H), latently infected (L) and infectious (I) leaf area over time, with L_ρ and L_σ denoting the area index of latent lesions and I_ρ and I_σ denoting the infectious area index of the resistant and sensitive strains, respectively:

$$\frac{dH}{dt} = \gamma\left(A_{\text{Max}} - A\right) - \beta(t)H - \varepsilon\left(\frac{H}{A}\right)\left(C_\sigma + C_\rho + I_\sigma + I_\rho\right) \quad (5)$$

$$\frac{dL_\sigma}{dt} = \varepsilon_\sigma\left(\frac{H}{A}\right)\left(C_\sigma + I_\sigma\right) - \delta L - \beta(t)L_\sigma \tag{6}$$

$$\frac{dL_\rho}{dt} = \varepsilon_\rho\left(\frac{H}{A}\right)\left(C_\rho + I_\rho\right) - \delta L_\rho - \beta(t)L_\rho \tag{7}$$

$$\frac{dI_\sigma}{dt} = \delta_\sigma L_\sigma - \mu I_\sigma \tag{8}$$

$$\frac{dI_\rho}{dt} = \delta_\rho L_\rho - \mu I_\rho \tag{9}$$

The final fraction of the resistant strain in the population at crop senescence, $\theta_{\rho_{\text{End}}}$, is calculated as

$$\theta_{\rho_{\text{End}}} = \frac{I_\rho\left(t_{\beta_T}\right)}{I_\rho\left(t_{\beta_T}\right) + I_\sigma\left(t_{\beta_T}\right)} \tag{10}$$

2.2.3 | The Effect of the Fungicide on Pathogen Growth Rate

Fungicide effects on the two strains of *Z. tritici* are simulated in the model through a dose-dependent reduction of pathogen life cycle parameters ε (transmission rate; Equations 6 and 7) and δ (the rate at which latent lesions are converted to sporulating lesions; Equations 8 and 9), slowing the rate of increase of the pathogen population. Single-site fungicides are assumed to reduce both the transmission rate and the rate of conversion of latent infections to sporulating lesions. The infectious period of sporulating lesions is assumed to be unaffected by fungicides.

The fungicide dose at time t, $D(t)$, is expressed as a proportion of the maximum permitted individual dose (as defined on the product label), D_{Max}, and decays exponentially over time at rate v:

$$D(t) = D_0 e^{-v(t-t^*)} \tag{11}$$

where D_0 is the applied dose and t^* is the time of application. $D(t)$ is the 'effective dose' referred to in Section 1.

The fungicide reduces the pathogen life cycle parameters ε and δ by a fraction $f(t)$, which changes over time depending on the remaining fungicide dose, $D(t)$. The dose–response of $f(t)$ to $D(t)$ (Figure 1a,b) is described by a combination of an asymptote parameter, q, which is the maximum fractional reduction of the pathogen life cycle parameter (i.e., at infinite fungicide dose), and a curvature parameter, k, which defines how quickly the fractional reduction declines from the asymptote as $D(t)$ decreases:

$$f_\sigma(t) = q_\sigma\left(1 - e^{-k_\sigma D(t)}\right) \tag{12}$$

$$f_\rho(t) = q_\rho\left(1 - e^{-k_\rho D(t)}\right) \tag{13}$$

The asymptote parameters are denoted as q_σ and q_ρ, the curvature parameters as k_σ and k_ρ and the fractional reductions as $f_\sigma(t)$ and $f_\rho(t)$ for the sensitive and resistant strains, respectively. Each pathogen life cycle parameter affected by the fungicide is multiplied by $(1 - f(t))$ to represent the effect of the fungicide on the growth rate of the pathogen population. For example, the transmission rate of the sensitive strain at time t, $\varepsilon_\sigma(t)$, is calculated as

$$\varepsilon_\sigma(t) = \varepsilon_0\left(1 - f_\sigma(t)\right) = \varepsilon_0\left(1 - q_\sigma\left(1 - e^{-k_\sigma D(t)}\right)\right) \tag{14}$$

where ε_0 is the transmission rate in the absence of fungicides. It is assumed that there are no fitness costs of resistance. If $f_\sigma(t) > f_\rho(t)$, the density of the resistant strain will increase faster than the density of the sensitive strain, leading to an increase in the resistant strain fraction of the *Z. tritici* population.

2.2.4 | Types of Fungicide Resistance

We simulate two types of fungicide resistance based on the nature of the shift in sensitivity to the fungicide ('sensitivity shift'):

> Asymptote shift, ζ_q: parameter q is reduced relative to the sensitive strain.

> Curvature shift, ζ_k: parameter k is reduced relative to the sensitive strain.

We describe the level of sensitivity shift as a percentage. For example, a 50% asymptote shift means that $q_\rho = 0.5q_\sigma$. Partial resistance could take the form of either an asymptote shift or a curvature shift, or a combination of both. An asymptote shift means that the effect of any dose $D(t)$ against the resistant strain of the pathogen is reduced (Figure 1a). For a curvature shift, the instantaneous effect of a high dose of the fungicide may still be as potent, but at lower doses, it is less effective against the resistant strain than against the sensitive strain (Figure 1b). The biological significance of asymptote and curvature shifts is discussed in Section 1.

A 100% asymptote and a 100% curvature shift are functionally identical: both represent strains that are completely resistant to the fungicide at any dose $D(t)$. Otherwise, for a given percentage sensitivity shift, an asymptote shift will result in a more highly resistant strain than the same level of curvature shift (as can be seen by comparing Figure 1a,b). The difference in the fractional reduction of the sensitive strain compared to that of the resistant strain, $f_\sigma(t) - f_\rho(t)$, is greatest at a high fungicide dose $D(t)$ for asymptote shifts and greatest at an intermediate fungicide dose $D(t)$ for partial (< 100%) curvature shifts (Figure 1c,d).

2.2.5 | Calculation of the Selection Coefficient

We used the selection coefficient, s, to compare the rate of selection for the resistant strain in each scenario simulated (Milgroom and Fry 1988; van den Bosch, Oliver, et al. 2014). The selection coefficient is defined as the difference in fitness between the resistant and sensitive strains due to the application of the fungicide, where fitness is measured by the per capita rate of increase, r, of a population:

$$s = r_\rho - r_\sigma \tag{15}$$

where r_ρ and r_σ are the average per capita rates of increase of the resistant and sensitive strains, respectively, over the course of the growing season. We calculate total selection between the start of the simulation, t_0, and crop senescence, time t_{β_T}, denoting the total length of time simulated as T. Assuming exponential growth of the sensitive and resistant strains (in the absence of density dependence), the density of the sensitive strain and resistant strain at time t_{β_T}, denoted as $P_\sigma\left(t_{\beta_T}\right)$ and $P_\rho\left(t_{\beta_T}\right)$, respectively, can be calculated as

$$P_\sigma\left(t_{\beta_T}\right) = P_\sigma(0)e^{r_\sigma T} \tag{16}$$

$$P_\rho\left(t_{\beta_T}\right) = P_\rho(0)e^{r_\rho T} \tag{17}$$

where $P_\sigma(0)$ and $P_\rho(0)$ are the initial densities of the sensitive and resistant strain, respectively, at the start of the simulation.

Rearrangement of Equations (16) and (17) for r_σ and r_ρ and substitution of Equation (15) give

$$s = \frac{1}{T}\left(\ln\left(\frac{P_\rho\left(t_{\beta_T}\right)P_\sigma(0)}{P_\rho(0)P_\sigma\left(t_{\beta_T}\right)}\right)\right) \tag{18}$$

This can also be expressed in terms of the population fractions of the resistant and sensitive strains, θ_ρ and θ_σ at the beginning of the simulation and the end of the growing season:

$$s = \frac{1}{T}\left(\ln\left(\frac{\theta_{\rho_{\text{End}}}\theta_{\sigma_{\text{Start}}}}{\theta_{\rho_{\text{Start}}}\theta_{\sigma_{\text{End}}}}\right)\right) \tag{19}$$

2.3 | Model Implementation and Parameterisation

The model was implemented in MATLAB R2022b (The MathWorks Inc. 2022) using a built-in function 'ode45' for the solution of the ordinary differential equations.

The model was parameterised using data on GLAI and *Z. tritici* infection over time from field trials of wheat crops grown with and without fungicide application, recorded over 14 site-years between 1993 and 1995 in the United Kingdom, and corresponding daily weather data from meteorological stations within 1 km of the site (Milne et al. 2003, described as 'Data set 1'; te Beest et al. 2009). We refer to data from these trials as 'Dataset 1'. For each site-year, Dataset 1 includes data on four cultivars (Riband, Apollo, Slejpner and Haven), with four replicates per cultivar.

We chose to follow previous models (Elderfield et al. 2018; Hobbelen, Paveley, and van den Bosch et al. 2011; van den Berg et al. 2013) in parameterising the model on a zero-degree days scale. Weather data for the sites were used to calculate both the thermal time (degree days base 0°C) and photo-vernal-thermal time (base 1°C) since sowing (Milne et al. 2003; Weir et al. 1984) corresponding to each observation date. The photo-vernal-thermal time gave a more consistent profile for the timings of the upper canopy growth and senescence than thermal time (see Figure A.1.2 in File S1 for further details). Using linear regression, we derived a relationship between thermal time and photo-vernal-thermal time, t_{pvt}, and used this to convert t_{pvt} to the average thermal time in zero-degree days, t:

$$t = 1.204t_{pvt} + 778.6 \tag{20}$$

Dataset 1 was used to estimate the average number of zero-degree days per day, z.

We assumed that data from field plots that received a fungicide programme designed to provide full protection against disease (Milne et al. 2003) are representative of canopy growth in the absence of disease. We used these data to estimate the parameters controlling the growth and senescence of the wheat canopy: t_0, t_{β_0}, t_{β_T}, A_{Max}, γ, τ, φ and ω (defined in Section 2.2.1). The mean GLAI of the top three leaves at each observation time point was calculated for each site-year from data from all four cultivars and replicates in Dataset 1. The parameters were fitted to data pooled from six site-years with maximum observed GLAI ranging from 3.76 to 4.90 (Cambridgeshire-1994, Devon-1994, Devon-1995, Kent-1995, Norfolk-1994, Norfolk-1995), using least-squares optimisation (lsqcurvefit, MATLAB R2022b; further details in File S1). Model zero-degree days were mapped to growth stages on Zadoks' scale (Zadoks et al. 1974), based on the fitted values of t_0, t_{β_0}, t_{β_T} and the estimated phyllochron length (see File S1 for further details).

We estimated *Z. tritici* life cycle parameters δ, μ and λ (defined in Section 2.2.2) based on data from a literature search (Table 2). In combination with C_0 (Equation 4) and ε_0 (Equations 6, 7 and 14), these parameters describe the infection of crop by *Z. tritici* in the absence of a fungicide. We estimated values for C_0 and ε_0 using data on STB epidemic progress (% severity) (Dataset 1) on untreated plots on which the maximum severity of the STB epidemic exceeded 5% and the maximum cumulative severity of yellow rust, brown rust and powdery mildew did not exceed 15%. Data from cultivars that were considered moderately resistant at the time the trials were carried out were used to estimate ε_0. Data from six site-years (Devon-1994, Devon-1995, Hampshire-1995, Herefordshire-1994, Herefordshire-1995, Kent-1994) fitted these criteria. We fitted separate values of C_0 and ε_0 for each site-year-cultivar combination using least-squares optimisation and calculated the average of these values (further details in File S1).

We used data from AHDB Fungicide Performance trials (AHDB 2024a) on the observed dose–response of STB severity to fluxapyroxad and isopyrazam from 2011 to 2012 (Dataset 2) to estimate indicative values of q_σ and k_σ for SDHI fungicides (see File S1 for further details), using an estimate of ν based on a literature search (Table 2).

2.4 | Model Simulations of Dose Splitting

We investigated the impact of dose splitting on selection for resistant strains with either an asymptote shift or a curvature shift (either partial or complete resistance) for a range of values of the fungicide parameters q_σ, k_σ and ν and of the pathogen transmission rate, ε_0 (Table 1). We compared selection for the resistant

TABLE 1 | List of parameter values simulated.

Parameter	Description	Values simulated
D_{Total}	Total fungicide dose applied to the upper leaf canopy	1, i.e. D_{Max}
$\theta_{\rho_{\text{Start}}}$	Initial fraction of the inoculum C that is resistant	0.01
q_σ	Asymptote of fungicide dose–response (sensitive strain)	0.05, 0.1, 0.25, 0.5, 0.75, 0.8, 0.95, 1
k_σ	Curvature of fungicide dose–response (sensitive strain)	0, 0.25, 0.5, 0.75, 1, 1.5, 2, 4, 5, 7.5, 10, 15, 20, 30
ν	Decay rate (t^{-1})	0.01605, 0.00802, 0.00401
ζ_q	Asymptote shift of the resistant strain	0, 1, 5, 10, 25, 50, 75, 90, 100
ζ_k	Curvature shift of the resistant strain	0, 1, 5, 10, 25, 50, 75, 90, 100
ε_0	Transmission rate	0.01055, 0.0211, 0.0422, 0.0800
GS32	Timing of GS32 application (zero-degree days)	1495
GS39	Timing of GS39 applications (zero-degree days)	1653

Note: All combinations of q_σ, k_σ and ν values simulated for each value of ζ_q and ζ_k listed.

strain following a single application of the fungicide at full label rate, D_{Max}, at either growth stage 32 (GS32) or GS39, to selection for the resistant strain following a 'split dose' application of $0.5D_{\text{Max}}$ at both GS32 and GS39. In all simulations, the total dose applied to the upper leaf canopy, D_{Total}, was equal to D_{Max}.

The foliar concentration half-lives of fungicide products can be very variable depending on the crop and environmental conditions (Fantke et al. 2014). We simulated three values of ν (Table 1), equivalent to foliar half-lives of 3, 6 and 12 days; SDHI fungicides such as fluxapyroxad, penthiopyrad and fluopyram have an average half-life of approximately 6 days (Fantke et al. 2014; He et al. 2016; Noh et al. 2019). Figure 2 illustrates the effect of the decay rate on the simulated fungicide dose $D(t)$ and fractional reduction $f(t)$ over time following single and split dose applications.

We included very low and high values of parameters q_σ and k_σ in the analysis to understand the extremes of the range of possible effects of dose splitting. In practice, these parameter values are unlikely in a commercially available fungicide: fungicides with very low values of q_σ or k_σ would not be effective, while very high values are more likely to be associated with an unacceptable toxicity profile. We compared our results to those obtained using our fitted parameter values for SDHI fungicides to understand the most likely range of effects of dose splitting on selection for resistance to commercial fungicides.

We assumed that $\theta_\rho(0) = 0.01$, that is, 1% of the inoculum initiating the epidemic was the resistant *Z. tritici* strain, while the remaining 99% of the population was sensitive to the fungicide. The simulations were run for a single growing season from the start of the leaf growth of the upper canopy, t_0, to complete canopy senescence, t_{β_T}. For each combination of parameter values simulated, the selection coefficient for the resistant strain, s, was calculated (Equation 19). The percentage change in the selection coefficient due to dose splitting, η, was then calculated as

$$\eta = 100 \times \frac{\left(s_{\text{Split}} - s_{\text{Single}}\right)}{s_{\text{Single}}} \tag{21}$$

where s_{Single} is the selection coefficient for a single application at D_{Total} and s_{Split} is the selection coefficient for the resistant strain for a split dose application.

3 | Results

3.1 | Model Parameterisation

The fitted model parameters are summarised in Table 2. The model fit to observed GLAI in the absence of disease was good (Figure 3a; $n = 76$, $R^2 = 76.9\%$, RMSE = 0.76). For the cultivar-site-year combinations used to fit ε_0, the transmission rate in the absence of fungicide, the overall fit to observed disease severity progress was excellent ($n = 293$, $R^2 = 88.4\%$, RMSE = 2.8%); fitted values of ε_0 ranged from 0.0136 to 0.0364, with a mean value of 0.0211. In the absence of a fungicide, the model predicts STB severity of 9.5% (Figure 3b) at GS75 (medium milk), which is approximately equivalent to the expected average severity on a cultivar with an AHDB resistance rating of 6 (AHDB 2024b).

3.2 | Effect of Dose Splitting on Selection for Fungicide Resistance

For the range of parameter values simulated (Table 1), we show results for both the overall magnitude of selection, measured by the selection coefficient s (Section 2.2.5), and the percentage change in selection due to dose splitting, η (Equation 21). When describing the baseline level of efficacy of a fungicide in Sections 3.2.1 and 3.2.2, we refer to the dose–response against the sensitive strain, notated as q_σ and k_σ for the asymptote and curvature parameter, respectively. For a resistant strain with an asymptote shift, $\zeta_q > 0$ but no curvature shift, that is, $\zeta_k = 0$, note that $k_\rho = k_\sigma$. For a resistant strain with a curvature shift $\zeta_k > 0$ but no asymptote shift, $q_\rho = q_\sigma$.

3.2.1 | Magnitude of Selection

The magnitude of selection for fungicide resistance, measured by the selection coefficient s, increased for both single and

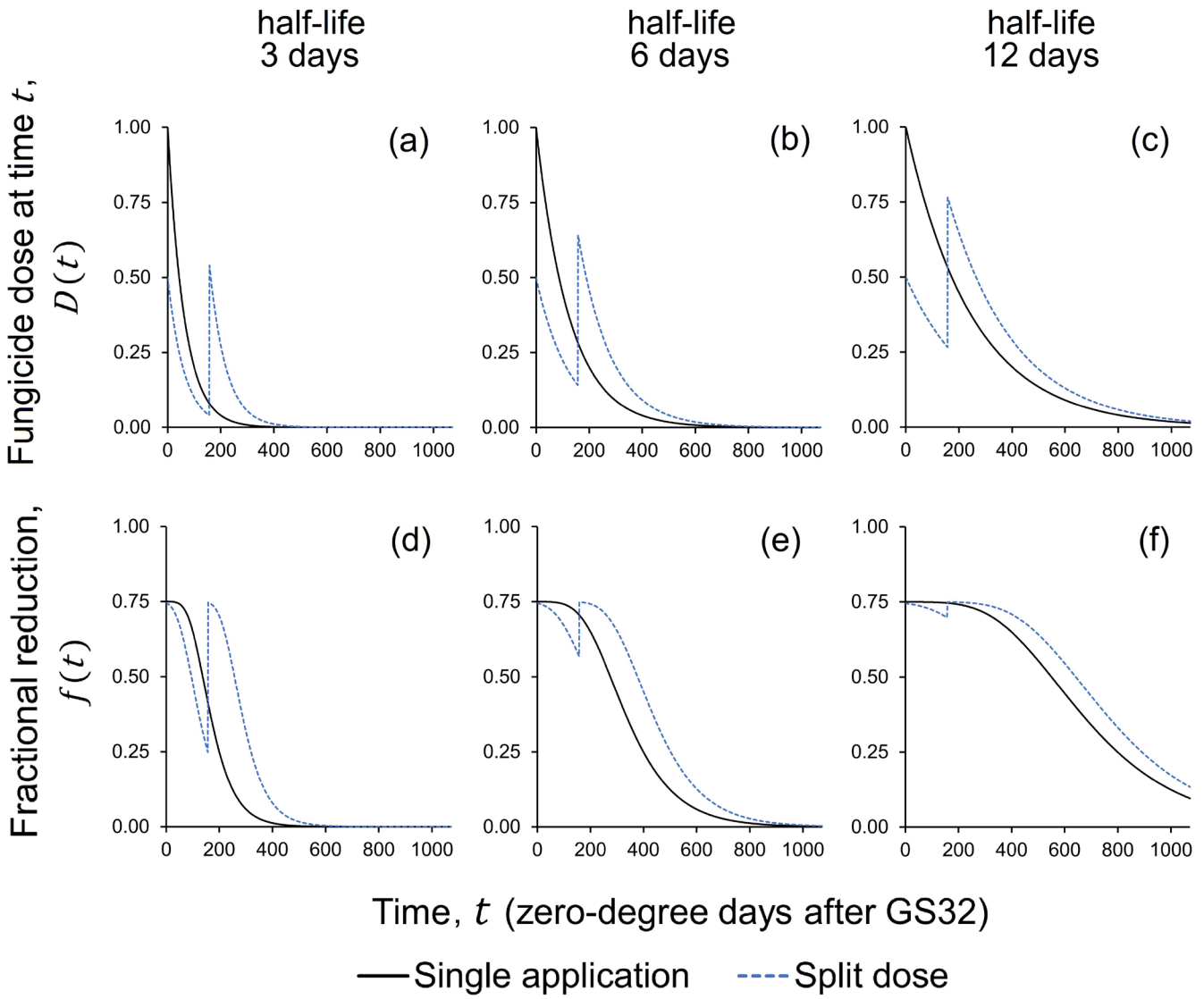

FIGURE 2 | Effect of decay rate ν on the simulated fungicide dose, $D(t)$, and fractional reduction, $f(t)$, over time following single (solid black line) and split dose (blue dashed line) applications of a fungicide with $q = 0.75, k = 10$. Panels (a), (b) and (c) show $D(t)$ for $\nu = 0.016\ t^{-1}$, $\nu = 0.008\ t^{-1}$ and $\nu = 0.004\ t^{-1}$, corresponding to foliar half-lives of 3, 6 and 12 days, respectively. Panels (d), (e) and (f) show $f(t)$ for $\nu = 0.016\ t^{-1}$, $\nu = 0.008\ t^{-1}$ and $\nu = 0.004\ t^{-1}$, respectively. [Colour figure can be viewed at wileyonlinelibrary.com]

split dose fungicide applications with increasing values of the asymptote parameter, q_σ, curvature parameter, k_σ, asymptote shift, ζ_q, curvature shift, ζ_k, or transmission rate, ϵ_0, and with decreasing values of the decay rate, ν (Figure 4, Figure A.2.1 in File S2). This means that a strain with resistance against a highly effective fungicide (with high values of q_σ, k_σ and a relatively low value of ν) would spread more quickly if the fungicide was applied, compared to a strain with resistance against a fungicide with lower efficacy. The greater the effect of a fungicide on the growth rate of the sensitive strain, the greater the maximum magnitude of the cumulative difference in growth rates between the resistant and sensitive strains when the fungicide is applied. More highly resistant strains (higher values of ζ_q or ζ_k) will also spread more quickly, as they have higher growth rates in the presence of a fungicide relative to the sensitive strain.

As noted in Section 2.2.4, either a 100% asymptote shift or 100% curvature shift leads to a strain that is completely resistant to the fungicide at any dose $D(t)$, and an identical value of s for a given combination of q_σ, k_σ and ν. For a given sensitivity shift percentage less than 100% (e.g., 50% or 90%), s is higher for an asymptote shift than for the same level of curvature shift, as the asymptote shift corresponds in a more highly resistant strain, leading to a greater cumulative difference in growth rates between the resistant and sensitive strain when fungicide is applied.

For partial and complete asymptote shifts, s was consistently higher for split-dose applications than for single applications.

3.2.2 | Effect of Dose Splitting on Selection for Resistance, η

The values of the asymptote parameter, q_σ, and asymptote shift, ζ_q, have very little impact on the percentage change in the selection coefficient s (η in Equation 21) as a result of dose splitting (Figure 5). q_σ also has very little impact on η for a curvature shift

TABLE 2 | Fitted parameter values.

Parameter	Definition	Units	Fitted value	Source
t_0, GS31	Timing of the start of growth of leaf 3	t	1396	[a]
GS32	Timing of GS32: leaf 3 fully emerged	t	1495	[a]
GS37	Timing of GS37: leaf 2 fully emerged	t	1574	[a]
GS39	Timing of GS39: flag leaf fully emerged	t	1653	[a]
t_{β_0}, GS61	Timing of anthesis and start of leaf 3 senescence	t	1891	[a]
t_{β_T}, GS87	Timing of end of grainfill and complete senescence of wheat canopy	t	2567	[a]
A_{Max}	Maximum leaf area index of top three leaves of the wheat canopy	—	4.438	[a]
γ	Growth rate of leaf area	t^{-1}	0.0082	[a]
τ	Coefficients controlling the rate of senescence over time, in relation to the length of time after the onset of senescence	t^{-1}	0.0028	[a]
φ		t^{-1}	0.704	[a]
ω		t^{-1}	0.314	[a]
$1/\delta$	Average latent period	t	350	[b]
$1/\mu$	Average infectious period	t	600	[c]
C_0	Initial density of infectious lesions on the lower leaves	—	0.0144	[a]
λ	Rate at which $C(t)$ decreases	t^{-1}	0.00897	[d]
ε_0	Transmission rate	—	0.0211	[a]
z	Number of zero-degree days per day	t	14.4	[a]
q_σ	Asymptote parameter for an SDHI fungicide (against sensitive strain)	—	0.569	[e]
k_σ	Curvature parameter for an SDHI fungicide (against sensitive strain)	—	9.9	[e]
ν	Decay rate for an SDHI fungicide	t^{-1}	0.00802	[f]

Note: Time, t, is measured in degree days (base 0°C) after sowing.
[a]Estimate based on 'Data set 1' from Milne et al. (2003).
[b]Shaw (1990); Suffert et al. (2013).
[c]Boixel (2020); Eyal (1971).
[d]Hobbelen, Paveley, and van den Bosch (2011).
[e]Estimate based on data from AHDB Fungicide Performance field trials.
[f]Fantke et al. (2014); He et al. (2016); Noh et al. (2019).

(Figure A.2.2, in File S2). This is because q_σ and ζ_q do not affect the length of time for which there is a difference in the level of control exerted by single and split dose applications. The curvature parameter, k_σ, and the decay rate, ν, together control the value of η, in combination with the curvature shift, ζ_k, where relevant (Figure 6). The transmission rate, ε_0, only has a small effect on the value of η (Figure A.2.3 in File S2).

For any asymptote shift, dose splitting increased selection for resistance. The value of η for an asymptote shift varied from $<5\%$ to 40%, depending on the values of k_σ and ν (Figure 6a–c). Our results suggest that splitting the dose of a solo SDHI across two applications rather than making a single application at full dose rate could increase selection for a strain with an asymptote shift to the SDHI by approximately 20%.

For curvature shifts, η varied from −20% to 80% (Figure 6d–f), indicating that dose splitting can reduce selection for partially resistant strains in some cases, but in other cases it may lead to a large increase in selection for resistance, dependent on the values of k_σ, ν and ζ_k. The value of η increased with the curvature parameter, k_σ, reaching an asymptote at high values of k_σ when the fungicide half-life was short (Figure 6d). For longer fungicide half-lives, the value of η initially increased with k_σ to a maximum, then decreased at very large values of k_σ (Figure 6f). For larger curvature shifts, ζ_k, the η-values approach the curves for asymptote shifts (Figure 6a–c). For smaller curvature shifts, $\zeta_k < 50\%$, η initially increased with k_σ, to a maximum at approximately $5 \leq k_\sigma \leq 10$, and then decreased again for larger values of k_σ. For small curvature shifts, ζ_k, large curvature parameters, k_σ, and longer fungicide half-lives, η approached zero or even became negative. Our results suggest that dose splitting of a solo SDHI application would increase selection for a strain with a curvature shift to the SDHI by approximately 20%–35%, with smaller curvature shifts falling towards the upper end of this range.

Dose splitting will increase selection for resistance if it leads to a larger difference in the growth rates of the sensitive strain and resistant strain for a longer time than a single application, that is, if it increases the overall sum of the differences in fractional reduction, $\sum_{t=0}^{T}\left(f_\sigma(t) - f_\rho(t)\right)$. For an asymptote shift,

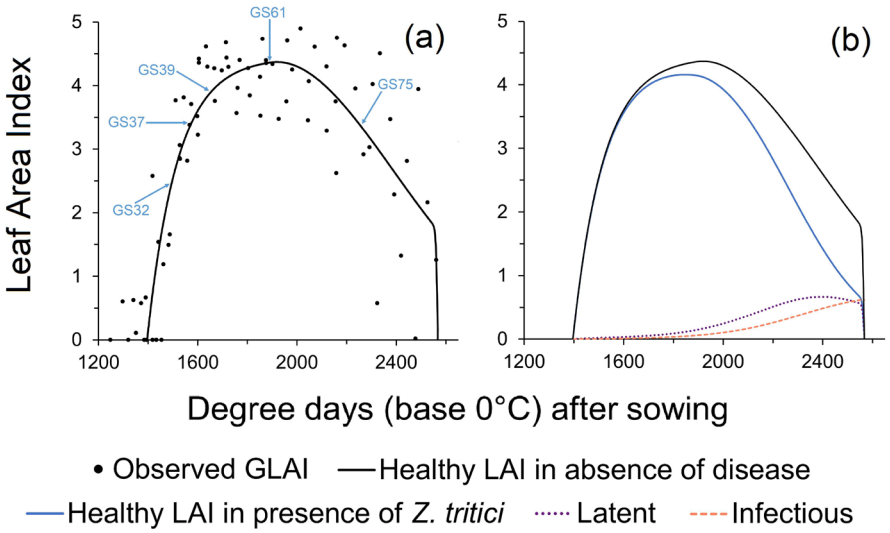

FIGURE 3 | Model simulation of the growth, senescence and infection by *Zymoseptoria tritici* of the upper wheat canopy. (a) Model simulation of healthy leaf area index (LAI) in the absence of disease (solid line) and observed green leaf area index (GLAI) measurements used for parameterisation of wheat canopy (points) ($n = 76$, from six sites from Dataset 1). The simulated timings of growth stages 32, 37, 39, 61 and 75 are indicated (blue arrows). (b) Model simulation of healthy (not latently infected) LAI in the presence of *Z. tritici*, latently infected LAI and infectious LAI for an average untreated epidemic of Septoria tritici blotch in the UK. [Colour figure can be viewed at wileyonlinelibrary.com]

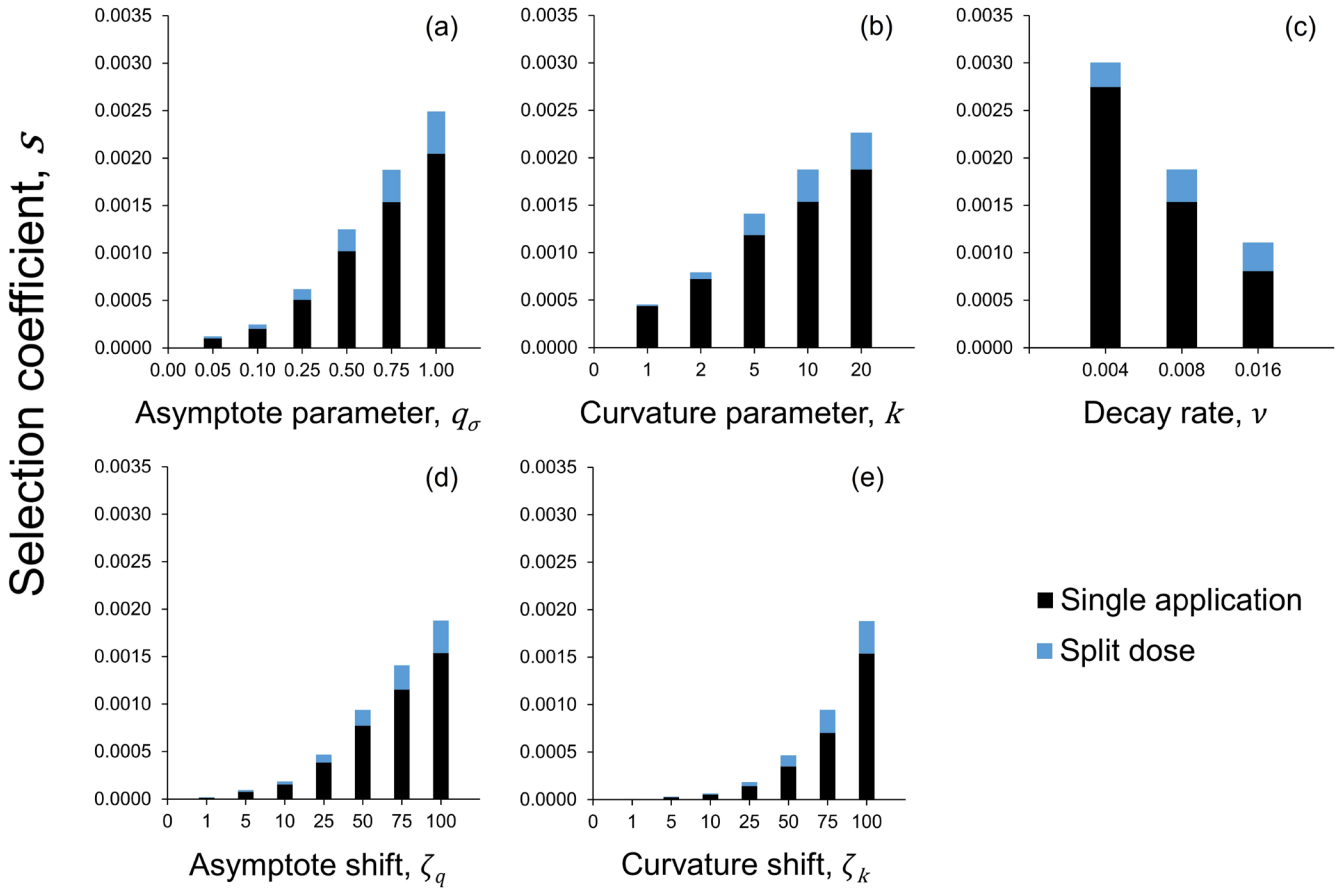

FIGURE 4 | Effect of fungicide properties and resistance type on the magnitude of selection for a resistant strain. Variation in selection coefficient, s, with (a) asymptote parameter, q_σ; (b) curvature parameter, k; (c) decay rate, ν; (d) asymptote shift, ζ_q; and (e) curvature shift, ζ_k. Only one parameter varied at a time: $\nu = 0.008$ for (a), (b), (d) and (e); $q_\sigma = 0.75$ for (b)–(e); $k_\sigma = 10$ for (a) and (c)–(e); $\zeta_q = 100\%$ for (a)–(c) and 0% for (e); $\zeta_k = 0\%$ for (a)–(d). s measures the magnitude of selection for a resistant strain. [Colour figure can be viewed at wileyonlinelibrary.com]

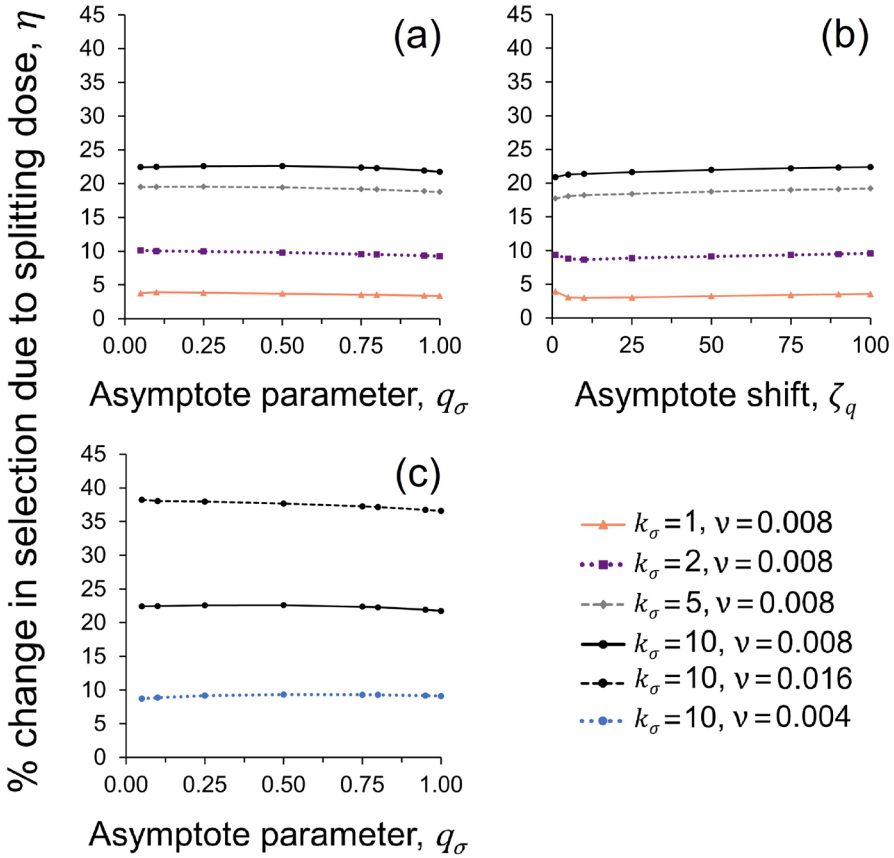

FIGURE 5 | Negligible effect of asymptote parameter, q_σ, and asymptote shift, ζ_q on η, the percentage change in selection due to dose splitting. Variation in η with (a) q_σ and (b) ζ_q for $k_\sigma = 1$, 2, 5 and 10. (c) Variation in η with q_σ for decay rates $\nu = 0.004\ t^{-1}$, $0.008\ t^{-1}$ and $0.016\ t^{-1}$. η is measured as the percentage change in selection as a result of splitting a total fungicide dose D_{Total} over two applications of $0.5D_{Max}$ at GS32 and GS39. [Colour figure can be viewed at wileyonlinelibrary.com]

the maximum difference in the growth rates of the sensitive strain and the resistant strain occurs at high fungicide doses, $D(t)$, for which the fractional reduction $f_\sigma(t)$ is close to the maximum (as defined by the asymptote q_σ) (Figure 1c). For a curvature shift, dose–response curves for sensitive and resistant strains converge at high values of $D(t)$. The maximum difference in the fractional reduction and resulting growth rates of the sensitive strain and a resistant strain with a curvature shift occurs at intermediate fungicide dose $D(t)$ (Figure 1d). As discussed by Taylor and Cunniffe (2023b), the effect of dose–response convergence on selection must be considered not only at the applied dose, but across the full time span of fungicide decay. Dose splitting increases the length of time that the pathogen is exposed to intermediate fungicide doses, which therefore increases $\sum_{t=0}^{T}\left(f_\sigma(t) - f_\rho(t)\right)$. The results in Figure 6 can be understood by considering how the values of k_σ, ν and ζ_k affect the size and duration of the difference in the growth rates of the sensitive and resistant strain, for single and split dose applications.

3.2.2.1 | Effect of Decay Rate, ν. For both asymptote shifts and curvature shifts, η was higher for larger values of ν (Figure 6). If the decay rate is high, the effect of a single application dissipates quickly, so a split dose application is likely to double the exposure time. If the decay rate is low, the effect of a single application at full dose rate will last for longer, so there is less difference in exposure time compared to the split dose application.

3.2.2.2 | Why Does η Increase With k_σ for Asymptote Shifts?. For small values of the curvature parameter k_σ (approx. <4), the maximum reduction of the sensitive strain life cycle parameters is only achieved at a high fungicide dose, $D(t)$, and the fractional reduction reduces quickly as $D(t)$ decreases (Figure A.2.4a in File S2). Therefore, the higher maximum dose applied in the single application initially achieves a much higher fractional reduction than the split dose application. Larger corresponding differences in the growth rates of the resistant and sensitive strain partially counterbalance the increased selection from the increased exposure time in the split dose application. The rate of selection from either a single or split dose application is therefore relatively similar for small values of k_σ, resulting in small values of η.

As k_σ increases, the fractional reduction remains close to the maximum fractional reduction even at lower fungicide doses $\leq 0.5\ D_{Max}$, so at lower values of $D(t)$, differences in the growth rates of the resistant and sensitive strain are similar to the difference at the full dose rate (Figure A.2.4b in File S2). The effect of the increased exposure time from the split dose therefore dominates at higher values of k_σ, resulting in higher values of η.

3.2.2.3 | Why Does η Exhibit a Maximum vs. k_σ for Asymptote Shifts When ν Is Low?. If k_σ is large and ν is low, the effect of a single application persists close to the maximum fractional reduction for a long time (Figure 2f;

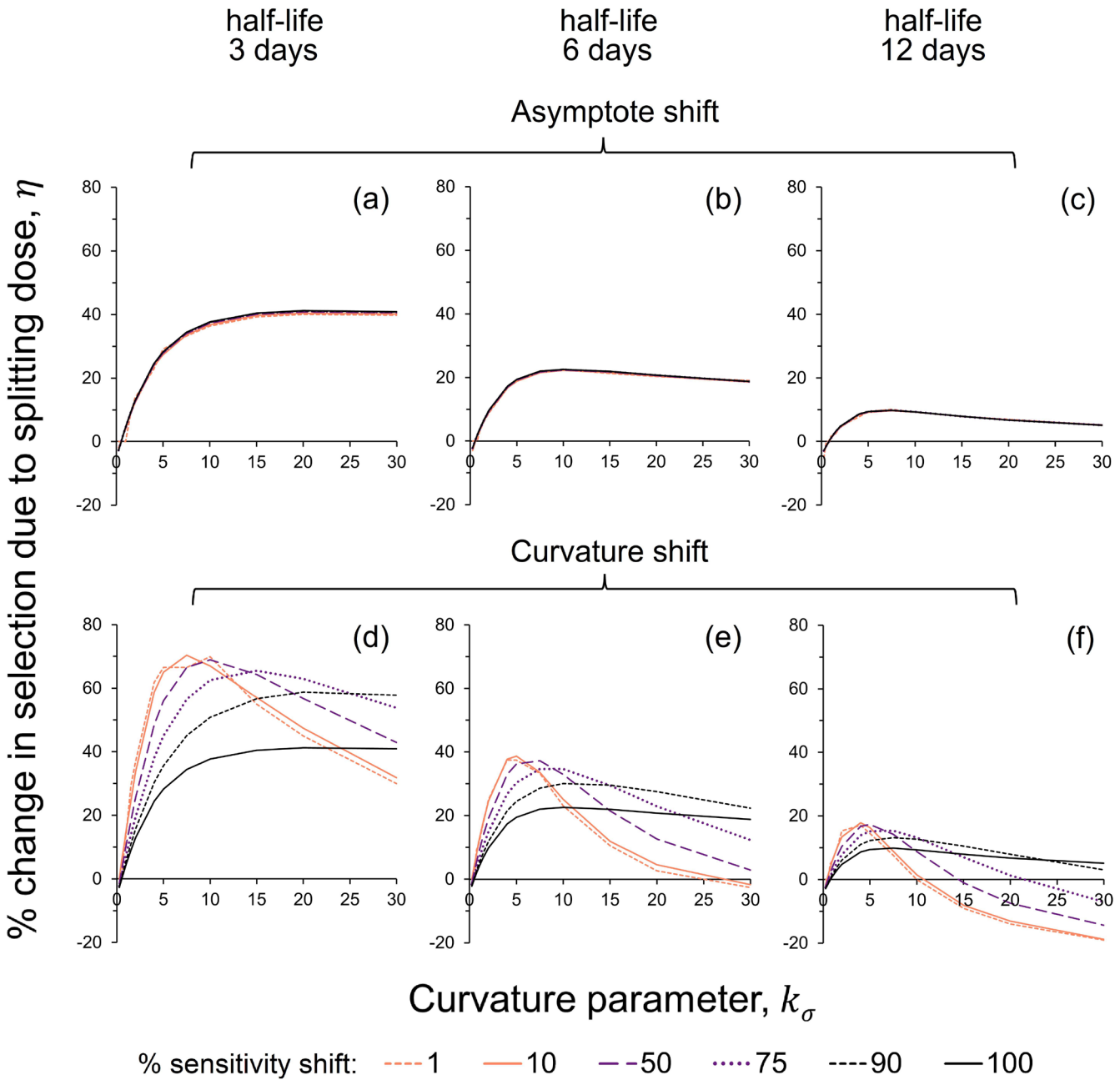

FIGURE 6 | Percentage change in selection, η, as a result of dose splitting for a range of parameter values: Curvature parameter, k_σ, decay rate, ν, and levels of sensitivity shift, ζ_q and ζ_k. Dose splitting simulated as two applications of $0.5D_{Max}$ at GS32 and GS39, compared to a single application of D_{Max} at GS32. Panels (a), (b) and (c) show the effect of k_σ on η for a resistant strain with an asymptote shift, ζ_q, for fungicide decay rates $\nu = 0.016\ t^{-1}$, $\nu = 0.008\ t^{-1}$ and $\nu = 0.004\ t^{-1}$, corresponding to foliar half-lives of 3, 6 and 12 days, respectively. Panels (d), (e) and (f) show the effect of k_σ on η for a resistant strain with a curvature shift, ζ_k, for fungicide decay rates $\nu = 0.016\ t^{-1}$, $\nu = 0.008\ t^{-1}$, and $\nu = 0.004\ t^{-1}$, respectively. Results shown for asymptote parameter $q_\sigma = 0.5$; the effect of q_σ on η is very small (see Figure 5). [Colour figure can be viewed at wileyonlinelibrary.com]

Figure A.2.4c in File S2), which shifts the point at which there is a large difference in the fractional reduction from the single application and the split dose application later in the season. Because canopy senescence begins to restrict the growth rates of both the resistant and sensitive strains later in the season, the value of η is reduced relative to the maximum at intermediate values of k_σ and lower values of ν. However, the effect of dose splitting may still be larger than for small values of k_σ.

3.2.2.4 | Why Does η Increase With k_σ More for Curvature Shifts Than for Asymptote Shifts?. As k_σ increases, the dose–response curve for the sensitive strain becomes more steeply curved, resulting in a decrease in the fungicide dose $D(t)$ at which the difference $f_\sigma(t) - f_\rho(t)$ is maximised for a curvature shift. The larger the value of k_σ and the smaller the value of ζ_k, the lower the dose $D(t)$ at which the difference $f_\sigma(t) - f_\rho(t)$ is maximised (Figure 1; Figure A.2.4d–f in File S2), as resistant

strains with a small curvature shift are still well controlled at high fungicide doses.

For very small values of k_σ, the maximum difference in growth rates occurs at higher values of $D(t) > 0.5D_{Max}$, which may not be reached using a split dose application. The maximum difference in growth rates is reached by the higher dose rate of the single application, partially counterbalancing the increased exposure time from the split dose application. Therefore η is small for small values of k_σ for a curvature shift. For larger values of k_σ, the maximum difference in growth rates occurs at values of $D(t) < 0.5D_{Max}$. A split dose application keeps $D(t)$ close to the level that maximises $f_\sigma(t) - f_\rho(t)$ for longer. In combination with the effect of increased exposure time, a split dose application increases selection more for strains with a curvature shift than for strains with an asymptote shift for intermediate values of k_σ.

3.2.2.5 | Why Does η Become Negative for Small Curvature Shifts, Large Values of k_σ and Small Values of ν?. If k_σ is large and ζ_k is small, the maximum difference in growth rates occurs at very small values of $D(t) < 0.1D_{Max}$ (Figure A.2.4f in File S2). If the decay rate, ν, is also small, low values of $D(t)$ are not reached for a split dose application until late in the season, when canopy senescence restricts the growth rates of both the resistant and sensitive strains, leading to low or even negative values of η for large values of k_σ combined with small values of ν and small values of ζ_k.

It is important to note that our results do not suggest that there would be no selection for resistance in cases where η was close to 0 or even negative: on the contrary, selection for resistance will usually be strong in cases with large values of k_σ and small values of ν (Figure 4), as resistance against a very effective fungicide gives a strong fitness advantage. However, in these cases dose splitting may have little effect on the strength of selection for resistance, or may even slightly decrease selection relative to a single application.

4 | Discussion

Dose splitting is likely to increase selection for both target-site and non-target-site resistance. Our results suggest that the percentage increase in selection due to dose splitting, η, is likely to be particularly large for resistance mechanisms that cause a curvature shift, where the effect of the fungicide is reduced at lower concentrations but not at high concentrations. These mechanisms could include non-target-site resistance, target-site overexpression and target-site mutations that affect fungicide competitive binding rates. Our results also support the hypothesis of van den Bosch, Oliver, et al. (2014) that dose splitting will increase selection for target-site mutations that cause an asymptote shift.

We show that the effects of dose splitting can be very variable for both target-site and non-target-site resistance. The largest increases in selection due to dose splitting are likely to occur for fungicides with a steeply curved dose–response curve (i.e., high values of k_σ) and a relatively short half-life (i.e., high values of the decay rate, ν). In these cases, dose splitting should be considered high risk for both target-site and non-target-site resistance.

Our analysis focused on dose splitting of a solo MoA, whereas resistance management guidelines recommend application in mixture with other MoAs; mixture may reduce selection for resistance and change the measured effects of dose splitting (Young et al. 2021). Where use of mixture requires 'splitting and mixing' due to limited numbers of effective MoAs for use in disease control, careful choice of mixture partners will be needed for fungicides for which dose splitting is high risk for resistance evolution. The use of alternative disease control measures as part of Integrated Pest Management (IPM) is likely to be particularly important in this context. Measures such as choice of crop cultivars with resistance to fungal diseases can reduce pathogen growth rates and/or enable a reduction in fungicide inputs, therefore reducing selection for fungicide resistance.

We found a small range of parameter values—fungicides with a large curvature parameter and a low decay rate—for which dose splitting could reduce selection for a resistant strain with a small curvature shift. However, these parameter values are relatively unlikely for a commercial fungicide, unless a high level of persistence could be achieved without associated environmental toxicity that would prevent regulatory approval. We used SDHI fungicides as an example of a commercial MoA currently available to growers. Our results suggest that dose splitting of an SDHI fungicide applied solo will increase selection for resistance by 20%–35%.

Our results suggest that variability in fungicide decay rates between years and sites due to differing environmental conditions is likely to contribute to the variable selection for SDH-mutants observed in field experiments on dose splitting (Paveley et al. 2020; Young et al. 2021). We modelled the effect of a 4-fold change in fungicide half-life, which is well within the maximum range observed in field conditions (Fantke et al. 2014). Our results suggest that for a fungicide with $k_\sigma = 10$, the variation in decay rates could account for the variation in the percentage effect of dose splitting on selection, η, in the range 10%–40% for an asymptote shift, or 0%–70% for a curvature shift (Figure 6b,e). The statistical power or field trials to detect the lower end of this range may be limited due to experimental noise, but our results confirm that dose splitting tends to increase selection for resistance.

There is a strong covariance between the fitted values of k_σ, q_σ and ν for the SDHI fungicide, increasing uncertainty in the estimation of these parameters and the consequences of dose splitting. We also assumed that k_σ and q_σ were the same for the fractional reduction of the transmission rate and the rate of conversion from latent to infectious leaf tissue. Measures of fungicide foliar half-life for each trial, and laboratory investigation of the effects of different fungicide dose rates on life cycle parameters such as latent period, could provide valuable additional evidence to inform these parameter values.

In our study, we assumed negligible fitness costs of fungicide resistance, which is often the case (Hawkins and Fraaije 2018; Mikaberidze and McDonald 2015). However, fitness costs may sometimes suppress the growth rate of the resistant strain to a level below the growth rate of the sensitive strain. This can occur in the absence of fungicide, at low fungicide doses for an asymptote shift (Mikaberidze et al. 2017), or at high fungicide

doses for resistant strains with a small curvature shift. Fitness costs have been reported for some target-site and non-target-site mutations; conversely, resistant strains can also have increased virulence relative to wild-type strains (Dorigan et al. 2023).

We did not explicitly model polygenic resistance, where resistance is conferred by multiple genes and the degree of resistance can build up gradually over time as resistance mutations accumulate. At the population level, this process leads to a continuous distribution of resistance phenotypes across strains, with the average levels of resistance increasing over time as selection for resistance continues (Shaw 1989; Taylor and Cunniffe 2023a). The difference between the dose–response curves of partially resistant strains may be analogous to a small curvature shift in our model, meaning that dose splitting could strongly increase the rate of selection for polygenic resistance.

The variable effect of dose splitting complicates management of resistance evolving 'concurrently' to two or more MoAs at the same time. Use of mixtures may require splitting the total dose of a fungicide across two or more applications ('splitting and mixing') due to a limited number of MoA available. The balance between the effects of mixture and dose splitting on selection for resistance will change depending on fungicide properties and resistance type and strength. Previous modelling studies found that if it is necessary to combine two high-risk fungicides in a programme, mixture rather than alternation or concurrent use will generally present the best strategy to maximise the length of time that effective disease control can be maintained (Elderfield 2018; Hobbelen et al. 2013). However, Elderfield (2018) found that alternation may be a better strategy against strains with a small curvature shift. Experimental evolution in vitro on sensitive isolates of *Z. tritici* using mixtures of high-risk fungicides showed that the success of mixture in delaying resistance depended strongly on the mixture components, and some reduced-dose mixtures selected for generalist, multidrug resistance (MDR; Ballu et al. 2021). These results may be explained by our finding that dose splitting increases selection more for strains with a small curvature shift—representative of non-target-site resistance—than for strains with an asymptote shift. The optimal strategy to slow evolution of resistance to one fungicide may not be the optimal strategy for another fungicide. The efficacy of the fungicide programme is also a vital consideration, and, where relevant, the effects of sexual reproduction of the pathogen. We will use the insights into the drivers of variation in the effects of dose splitting presented in this paper to underpin further work investigating whether 'splitting and mixing' or alternation of two fungicides is a better strategy when concurrent evolution of resistance is a concern.

Because the balance between the effects of mixture and dose splitting on selection for resistance will differ for asymptote and curvature shifts, this could introduce trade-offs between tactics to reduce selection for large, target-site asymptote shifts and alternative tactics to limit incrementally increasing levels of resistance due to mechanisms that cause a curvature shift. These trade-offs appear to occur in weed management, where the use of herbicide mixtures is associated with a lower prevalence of target-site resistance but a higher prevalence of metabolic resistance (Comont et al. 2020). Fungicide resistance management strategies have tended to focus on large asymptote shifts associated with target-site mutations, as these can lead to a rapid loss of fungicide efficacy, for example, as experienced in QoI fungicides for multiple pathogens (Grimmer et al. 2015). Due to their large effects, target-site mutations that result in an asymptote shift are more likely to be quickly identified and studied than individual non-target-site resistance mechanisms that may be overlooked due to the small effects of each gene (Hu and Chen 2021). However, in combination with target-site resistance, non-target-site mechanisms may contribute to highly resistant MDR strains (Omrane et al. 2017). Synergistic interactions between resistance mechanisms could enhance the overall impact of non-target-site resistance: for example, increased efflux reduces the cellular fungicide concentration and could therefore increase the effect of a target-site mutation that causes a partial curvature shift. Wherever possible, tactics should be chosen for their effectiveness against both target-site and non-target-site resistance.

Acknowledgements

This research was funded by AHDB (project 21120062). Rothamsted Research receives strategic funding from the Biotechnology and Biological Sciences Research Council of the United Kingdom. A.E.M. acknowledges support from the Growing Health Institute Strategic Programme (BBS/E/RH/230003C).

Conflicts of Interest

The authors declare no conflicts of interest.

Data Availability Statement

Dataset 1: Data sharing is not applicable to this dataset as no new data were created or analysed in this study. Dataset 2: These data are available from the Agriculture and Horticulture Development Board (AHDB). Restrictions apply to the availability of these data, which were used under licence for this study. A summarised version of the data used is available at https://ahdb.org.uk/knowledge-library/a-guide-to-fungicide-performance-in-wheat-barley-and-oilseed-rape and in File S1 (Figure A.1.5).

References

AHDB. 2024a. "*A Guide to Fungicide Performance in Wheat, Barley and Oilseed Rape*." https://ahdb.org.uk/knowledge-library/a-guide-to-fungicide-performance-in-wheat-barley-and-oilseed-rape.

AHDB. 2024b. "*Recommended Lists Disease Ratings*." https://ahdb.org.uk/recommended-lists-disease-ratings.

Ballu, A., A. Deredec, A.-S. Walker, and F. Carpentier. 2021. "Are Efficient-Dose Mixtures a Solution to Reduce Fungicide Load and Delay Evolution of Resistance? An Experimental Evolutionary Approach." *Microorganisms* 9: 2324.

Blake, J. J., P. Gosling, B. A. Fraaije, et al. 2018. "Changes in Field Dose–Response Curves for Demethylation Inhibitor (DMI) and Quinone Outside Inhibitor (QoI) Fungicides Against *Zymoseptoria tritici*, Related to Laboratory Sensitivity Phenotyping and Genotyping Assays." *Pest Management Science* 74: 302–313.

Boixel, A.-L. 2020. *Environmental Heterogeneity, a Driver of Adaptation to Temperature in Foliar Plant Pathogen Populations?* Université Paris-Saclay.

Comont, D., C. Lowe, R. Hull, et al. 2020. "Evolution of Generalist Resistance to Herbicide Mixtures Reveals a Trade-Off in Resistance Management." *Nature Communications* 11: 3086.

Cools, H. J., and B. A. Fraaije. 2013. "Update on Mechanisms of Azole Resistance in *Mycosphaerella graminicola* and Implications for Future Control." *Pest Management Science* 69: 150–155.

Corkley, I., B. Fraaije, and N. Hawkins. 2022. "Fungicide Resistance Management: Maximizing the Effective Life of Plant Protection Products." *Plant Pathology* 71: 150–169.

Dooley, H., M. W. Shaw, J. Mehenni-Ciz, J. Spink, and S. Kildea. 2016. "Detection of *Zymoseptoria tritici* SDHI-Insensitive Field Isolates Carrying the *SdhC* -H152R and *SdhD* -R47W Substitutions." *Pest Management Science* 72: 2203–2207.

Dorigan, A. F., S. I. Moreira, S. da Silva Costa Guimarães, V. Cruz-Magalhães, and E. Alves. 2023. "Target and Non-Target Site Mechanisms of Fungicide Resistance and Their Implications for the Management of Crop Pathogens." *Pest Management Science* 79: 4731–4753.

Elderfield, J. A. D. 2018. *Using Epidemiological Principles and Mathematical Models to Understand Fungicide Resistance Evolution*. PhD Thesis. University of Cambridge.

Elderfield, J. A. D., F. J. Lopez-Ruiz, F. van den Bosch, and N. J. Cunniffe. 2018. "Using Epidemiological Principles to Explain Fungicide Resistance Management Tactics: Why Do Mixtures Outperform Alternations?" *Phytopathology* 108: 803–817.

Eyal, Z. 1971. "The Kinetics of Pycnospore Liberation in *Septoria tritici*." *Canadian Journal of Botany* 49: 1095–1099.

Fantke, P., B. W. Gillespie, R. Juraske, and O. Jolliet. 2014. "Estimating Half-Lives for Pesticide Dissipation From Plants." *Environmental Science and Technology* 48: 8588–8602.

Fones, H., and S. Gurr. 2015. "The Impact of *Septoria tritici* Blotch Disease on Wheat: An EU Perspective." *Fungal Genetics and Biology* 79: 3–7.

Grimmer, M. K., F. van den Bosch, S. J. Powers, and N. D. Paveley. 2015. "Fungicide Resistance Risk Assessment Based on Traits Associated With the Rate of Pathogen Evolution." *Pest Management Science* 71: 207–215.

Hargrove, T. Y., Z. Wawrzak, D. C. Lamb, F. P. Guengerich, and G. I. Lepesheva. 2015. "Structure-Functional Characterization of Cytochrome P450 Sterol 14α-Demethylase (CYP51B) From *Aspergillus fumigatus* and Molecular Basis for the Development of Antifungal Drugs." *Journal of Biological Chemistry* 290: 23916–23934.

Hawkins, N. J., and B. A. Fraaije. 2018. "Fitness Penalties in the Evolution of Fungicide Resistance." *Annual Review of Phytopathology* 56: 339–360.

Hawkins, N. J., and B. A. Fraaije. 2021. "Contrasting Levels of Genetic Predictability in the Evolution of Resistance to Major Classes of Fungicides." *Molecular Ecology* 30: 5318–5327.

He, M., C. Jia, E. Zhao, et al. 2016. "Concentrations and Dissipation of Difenoconazole and Fluxapyroxad Residues in Apples and Soil, Determined by Ultrahigh-Performance Liquid Chromatography Electrospray Ionization Tandem Mass Spectrometry." *Environmental Science and Pollution Research* 23: 5618–5626.

Hobbelen, P. H. F., N. D. Paveley, B. A. Fraaije, J. A. Lucas, and F. van den Bosch. 2011. "Derivation and Testing of a Model to Predict Selection for Fungicide Resistance." *Plant Pathology* 60: 304–313.

Hobbelen, P. H. F., N. D. Paveley, R. P. Oliver, and F. van den Bosch. 2013. "The Usefulness of Fungicide Mixtures and Alternation for Delaying the Selection for Resistance in Populations of *Mycosphaerella graminicola* on Winter Wheat: A Modeling Analysis." *Phytopathology* 103: 690–707.

Hobbelen, P. H. F., N. D. Paveley, and F. van den Bosch. 2011. "Delaying Selection for Fungicide Insensitivity by Mixing Fungicides at a Low and High Risk of Resistance Development: A Modeling Analysis." *Phytopathology* 101: 1224–1233.

Hu, M., and S. Chen. 2021. "Non-Target Site Mechanisms of Fungicide Resistance in Crop Pathogens: A Review." *Microorganisms* 9: 502.

Huf, A., A. Rehfus, K. H. Lorenz, R. Bryson, R. T. Voegele, and G. Stammler. 2018. "Proposal for a New Nomenclature for *CYP51* Haplotypes in *Zymoseptoria tritici* and Analysis of Their Distribution in Europe." *Plant Pathology* 67: 1706–1712.

Kema, G. H. J., D. Yu, F. H. J. Rijkenberg, M. W. Shaw, and R. P. Baayen. 1996. "Histology of the Pathogenesis of *Mycosphaerella graminicola* in Wheat." *Phytopathology* 86: 777–786.

Kretschmer, M., M. Leroch, A. Mosbach, et al. 2009. "Fungicide-Driven Evolution and Molecular Basis of Multidrug Resistance in Field Populations of the Grey Mould Fungus *Botrytis cinerea*." *PLoS Pathogens* 5: e1000696.

Leroux, P., and A. Walker. 2011. "Multiple Mechanisms Account for Resistance to Sterol 14α-Demethylation Inhibitors in Field Isolates of *Mycosphaerella graminicola*." *Pest Management Science* 67: 44–59.

McDonald, B. A., F. Suffert, A. Bernasconi, and A. Mikaberidze. 2022. "How Large and Diverse Are Field Populations of Fungal Plant Pathogens? The Case of *Zymoseptoria tritici*." *Evolutionary Applications* 15: 1360–1373.

Mikaberidze, A., and B. A. McDonald. 2015. "Fitness Cost of Fungicide Resistance – Impact on Management." In *Fungicide Resistance in Plant Pathogens: Principles and a Guide to Practical Management*, edited by H. Ishii and D. Hollomon, 77–89. Springer Japan.

Mikaberidze, A., N. Paveley, S. Bonhoeffer, and F. van den Bosch. 2017. "Emergence of Resistance to Fungicides: The Role of Fungicide Dose." *Phytopathology* 107: 545–560.

Milgroom, M. G., and W. E. Fry. 1988. "A Simulation Analysis of the Epidemiological Principles for Fungicide Resistance Management in Pathogen Populations." *Phytopathology* 78: 565–570.

Milne, A., N. Paveley, E. Audsley, and P. Livermore. 2003. "A Wheat Canopy Model for Use in Disease Management Decision Support Systems." *Annals of Applied Biology* 143: 265–274.

Noh, H. H., J. Y. Lee, H. K. Park, et al. 2019. "Dissipation, Persistence, and Risk Assessment of Fluxapyroxad and Penthiopyrad Residues in Perilla Leaf (*Perilla frutescens* var. *japonica* Hara)." *PLoS One* 14: e0212209.

Omrane, S., C. Audéon, A. Ignace, et al. 2017. "Plasticity of the *MFS1* Promoter Leads to Multidrug Resistance in the Wheat Pathogen *Zymoseptoria tritici*." *mSphere* 2: e00393-17.

Parker, S. R., S. Welham, N. D. Paveley, J. Foulkes, and R. K. Scott. 2004. "Tolerance of Septoria Leaf Blotch in Winter Wheat." *Plant Pathology* 53: 1–10.

Patry-Leclaire, S., E. Neau, A. Pitarch, A.-S. Walker, and S. Fillinger. 2023. "Plasticity of the MFS1 Promotor Is not the Only Driver of Multidrug Resistance in *Zymoseptoria tritici*." *bioRxiv*. 2023.12.27.573052. [Preprint].

Paveley, N., B. Fraaije, F. van den Bosch, et al. 2020. "Managing Resistance Evolving Concurrently Against Two Modes of Action." In *Modern Fungicides and Antifungal Compounds*, edited by H. B. Diesing, B. Fraaije, A. Mehl, E. C. Oerke, H. Sierotzki, and G. Stammler, vol. IX, 141–146. Deutsche Phytomedizinische Gesellschaft.

Ponomarenko, A., S. B. Goodwin, and G. H. J. Kema. 2011. "*Septoria tritici* Blotch (STB) of Wheat." *Plant Health Instructor*. https://www.apsnet.org/edcenter/pdlessons/Pages/Septoria.aspx.

Rehfus, A., D. Strobel, R. Bryson, and G. Stammler. 2018. "Mutations in *Sdh* Genes in Field Isolates of *Zymoseptoria tritici* and Impact on the Sensitivity to Various Succinate Dehydrogenase Inhibitors." *Plant Pathology* 67: 175–180.

Shaw, M. W. 1989. "A Model of the Evolution of Polygenically Controlled Fungicide Resistance." *Plant Pathology* 38: 44–55.

Shaw, M. W. 1990. "Effects of Temperature, Leaf Wetness and Cultivar on the Latent Period of *Mycosphaerella graminicola* on Winter Wheat." *Plant Pathology* 39: 255–268.

Shaw, M. W., and D. J. Royle. 1989. "Estimation and Validation of a Function Describing the Rate at Which *Mycosphaerella graminicola* Causes Yield Loss in Winter Wheat." *Annals of Applied Biology* 115: 425–442.

Suffert, F., I. Sache, and C. Lannou. 2011. "Early Stages of *Septoria tritici* Blotch Epidemics of Winter Wheat: Build-Up, Overseasoning, and Release of Primary Inoculum." *Plant Pathology* 60: 166–177.

Suffert, F., I. Sache, and C. Lannou. 2013. "Assessment of Quantitative Traits of Aggressiveness in *Mycosphaerella graminicola* on Adult Wheat Plants." *Plant Pathology* 62: 1330–1341.

Taylor, N. P., and N. J. Cunniffe. 2023a. "Modelling Quantitative Fungicide Resistance and Breakdown of Resistant Cultivars: Designing Integrated Disease Management Strategies for Septoria of Winter Wheat." *PLoS Computational Biology* 19: e1010969.

Taylor, N. P., and N. J. Cunniffe. 2023b. "Coupling Machine Learning and Epidemiological Modelling to Characterise Optimal Fungicide Doses When Fungicide Resistance Is Partial or Quantitative." *Journal of the Royal Society Interface* 20: 20220685.

te Beest, D. E., M. W. Shaw, S. Pietravalle, and F. van den Bosch. 2009. "A Predictive Model for Early-Warning of Septoria Leaf Blotch on Winter Wheat." *European Journal of Plant Pathology* 124: 413–425.

The MathWorks Inc. 2022. *MATLAB Version: 9.13.0 (R2022b)*. MathWorks Inc.

Torriani, S. F., P. C. Brunner, B. A. McDonald, and H. Sierotzki. 2009. "QoI Resistance Emerged Independently at Least 4 Times in European Populations of *Mycosphaerella graminicola*." *Pest Management Science* 65: 155–162.

van den Berg, F., F. Bosch, and N. D. Paveley. 2013. "Optimal Fungicide Application Timings for Disease Control Are Also an Effective Anti-Resistance Strategy: A Case Study for *Zymoseptoria tritici* (*Mycosphaerella graminicola*) on Wheat." *Phytopathology* 103: 1209–1219.

van den Berg, F., N. D. Paveley, and F. van den Bosch. 2016. "Dose and Number of Applications That Maximize Fungicide Effective Life Exemplified by *Zymoseptoria tritici* on Wheat – A Model Analysis." *Plant Pathology* 65: 1380–1389.

van den Bosch, F., R. Oliver, F. van den Berg, and N. Paveley. 2014. "Governing Principles Can Guide Fungicide-Resistance Management Tactics." *Annual Review of Phytopathology* 52: 175–195.

van den Bosch, F., N. Paveley, F. van den Berg, P. Hobbelen, and R. Oliver. 2014. "Mixtures as a Fungicide Resistance Management Tactic." *Phytopathology* 104: 1264–1273.

Weir, A. H., P. L. Bragg, J. R. Porter, and J. H. Rayner. 1984. "A Winter Wheat Crop Simulation Model Without Water or Nutrient Limitations." *Journal of Agricultural Science* 102: 371–382.

Wollenberg, R. D., S. S. Donau, M. H. Taft, et al. 2020. "Undefeated—Changing the Phenamacril Scaffold Is Not Enough to Beat Resistant *Fusarium*." *PLoS One* 15: e0235568.

Young, C., T. Boor, I. Corkley, et al. 2021. "*Managing Resistance Evolving Concurrently Against Two or More Modes of Action to Extend the Effective Life of Fungicides*." AHDB Project Report No. 637. https://projectblue.blob.core.windows.net/media/Default/Research%20Papers/Cereals%20and%20Oilseed/2021/PR637%20final%20project%20report.pdf.

Zadoks, J. C., T. T. Chang, and C. F. Konzak. 1974. "A Decimal Code for the Growth Stages of Cereals." *Weed Research* 14: 415–421.

Supporting Information

Additional supporting information can be found online in the Supporting Information section.